NEES/E-Defense Base-Isolation Tests:
Interaction of Horizontal and Vertical Response

K.L. Ryan & N.D. Dao
University of Nevada, Reno

E. Sato & T. Sasaki
National Research Institute for Earth Science and Disaster Prevention

T. Okazaki
Hokkaido University

SUMMARY:
This is one of four papers reporting a NEES/E-Defense collaborative program on base-isolated buildings. A full-scale, five-story, two-by-two bay, steel moment-frame building was subjected to a number of bidirectional (XY) and bidirectional-plus-vertical (3D) ground motions using the E-Defense shake table. The building was tested under three different configurations: 1) base isolated with triple-friction-pendulum bearings (TPB), 2) base isolated with a combination of lead-rubber bearings (LRB) and cross-linear bearings (CLB), and 3) fixed-base. This paper discusses the influence of vertical excitation on the overall response of the building in each configuration, and introduces an explanation for the horizontal-vertical coupling that amplified the horizontal accelerations in 3D relative to XY excitation. Observed nonstructural damage was felt to be more closely correlated to vertical slab acceleration than horizontal floor acceleration, and the horizontal amplification did not compromise the effectiveness of the isolation system to completely protect the structural system from damage.

Keywords: base isolation, full scale testing, vertical excitation, triple pendulum bearing, lead-rubber bearing

1. INTRODUCTION

This is one of four papers reporting a collaborative program on base-isolated buildings conducted under the Memorandum of Understanding between the National Science Foundation (NSF), George Brown Jr. Network for Earthquake Engineering Simulation (NEES) program of the U.S. and the National Institute of Earth Science and Disaster Prevention (NIED) of Japan.

A large-scale, shake-table test program was conducted with a goal of promoting rapid spread of base isolation systems in Japan and the U.S. In this program, a full-scale, five-story, steel moment-frame building was subjected to a number of bidirectional and bidirectional-plus-vertical ground motions using the world's largest shake table, E-Defense. The building was tested under three different configurations: 1) base isolated with triple-friction-pendulum bearings (TPB), 2) base isolated with a combination of lead-rubber bearings (LRB) and cross-linear bearings (CLB), and 3) fixed-base. An overview of the test program with a comparative evaluation of the structural response in the three configurations is provided in Sasaki et al. (2012), while detailed isolation device response is provided in Okazaki et al. (2012). Nonstructural components and loose contents were installed on the fourth and fifth floors of the building, as reported by Soroushian et al. (2012). Finally, this paper reports on the influence of vertical excitation on the overall response of the structural system.

Prior test programs on base isolation have sometimes considered the influence of vertical excitation, although its evaluation has generally not been a primary objective. Programs that have directly evaluated the influence of vertical excitation have generally concluded that vertical excitation has no influence or very minor influence on the horizontal structural (e.g. Clark and Kelly 1990, Fenz and Constantinou 2008). Hwang and Hsu (2000) found that for a structure with an asymmetric configured isolation system, vertical acceleration significantly increased the structure floor accelerations. A few experimental studies have specifically evaluated secondary system response in isolated buildings by

mounting oscillators on a test frame to simulate the response of light equipment (Kelly and Tsai 1985, Juhn et al. 1992) or by focusing on evaluation of the floor accelerations and floor spectra (Wolff and Constantinou 2004). A recent E-Defense base-isolated hospital test program (Sato et al. 2011) and this NEES/E-Defense program are unique in their ability to observe the response of physical nonstructural components and furniture/equipment/loose items in a realistically configured structural system.

This paper describes the floor level acceleration demands observed in the specimen during the NEES/E-Defense test program, and outlines an explanation of the lateral-vertical coupling that was observed. Readers are referred to the overview companion paper (Sasaki et al. 2012) for the requisite background information about the experiment.

2. RELATION BETWEEN NONSTRUCTURAL SYSTEM PERFORMANCE AND VERTICAL EXCITATION

The test program incorporated a diverse selection of ground motions and shaking intensities, including vertical ground acceleration in excess of 1g. A complete test matrix is given in Ryan et al. (2012). In the description that follows, table motions that targeted specified input in x, y and z-directions are described as 3D, while table motions that targeted horizontal only shaking are described as XY. In general, the records were replicated by the shake table with increased intensity relative to the target in the short to intermediate period range. All peak ground acceleration values reported reflect the feedback values observed. The motions would have been reproduced more accurately by multi-step compensation with input reference modification techniques (Tagawa and Kajiwara 2007). However, the project team chose a non-compensation control method in favor of examining performance for a wide variety of input motions. Furthermore, uplift and re-contact of the bearings in TPBs and slippage of connection bolts of the LRBs, which induced acceleration impulses in the recorded structural response, may also have affected the measured table motions. All reported accelerations were processed with a low pass filter with a cutoff frequency of 50 Hz.

Throughout the test program, damage to certain nonstructural components and content disruption was observed that was closely correlated to vertical ground motion intensity. The most noteworthy damage observed was to the suspended ceiling system. Early in the program, the TPB configuration was subjected to 88% of 1994 Northridge at Rinaldi Rec. Sta. (RRS) with vertical peak table acceleration (V-PGA) exceeding 1g. Large numbers of ceiling panels were dislodged or fell, and in some locations, several adjacent rows of ceiling grid members fell. Similar damage was observed when RRS was repeated at the same intensity in the LRB/CLB configuration and with scale factors of 35% and 88% for horizontal and vertical input in the fixed-base configuration. Varying degrees of ceiling damage were observed throughout the test program for motions with substantial vertical components.

The ceiling damage appeared to be induced primarily by the significant vertical accelerations of the floor slabs from which the ceilings were hung. Figure 2.1 plots vertical accelerations recorded in the table, the columns, and the middle of the floor slab at the 5th and roof levels (corresponding to the 4th and 5th floor ceilings) for each of the 3 system configurations over the most intense part of 3D RRS record. Despite significant discrepancy in column accelerations, the vertical accelerations in the floor slabs are observed to be relatively similar for each system configuration, with peak intensities in the range of 6-8g. Figure 1 indicates that slab accelerations are dominated by single frequency vibration, which suggests that individual local vertical modes are activated at each floor level. The dominant slab vibration frequencies, confirmed by transfer function analysis, are about 10 Hz for the 5th floor slab and 7 Hz for the roof slab, and do not vary much as a function of building configuration. As a result, the vertical slab accelerations were unaffected by a near complete uplift excursion of the building in TPB configuration that transmitted very high frequency vertical accelerations to the columns [Fig. 2.1(a),(d)].

Overall, the ceiling system was found to be quite robust, and the test data suggests that threshold for damage under combined horizontal and vertical accelerations was quite large. A horizontal-vertical

acceleration "interaction diagram" for the 5th floor and roof slabs is shown in Fig. 2.2. These figures plot the peak horizontal acceleration recorded in any sensor (vector sum of x and y-components) against the peak vertical acceleration recorded in any sensor for each test motion, which did not necessarily occur at the same time. In these plots, XY and 3D ground excitations are differentiated, as well as excitations in each system (TPB, LRB/CLB and fixed-base). Imposed records that induced ceiling damage described as moderate or worse – evaluated independently at each floor level – are highlighted in black. Besides RRS, these motions included Sylmar and Tabas 80% (V-PGA = 0.58g and 0.63g) in the TPB isolated building; Vogtle 150%, Vogtle 175%, and Diablo Canyon 80% (V-PGA = 0.43g, 0.49g and 0.45g) in the LRB/CLB isolated building. Moderate ceiling damage was observed in a single XY record (Iwanuma 70% in the fixed-base building), which generated top level floor accelerations slightly greater than 1g. Based on Fig. 2.2(b), the threshold for damage to 5th floor ceilings was a combination of horizontal floor acceleration exceeding about 0.5g and vertical floor acceleration exceeding about 2.5g. However, only slight damage was observed in the 4th floor ceiling to the same records. A theory explaining the discrepancy between the two floors, which were configured differently, is described in Soroushian et al. (2012).
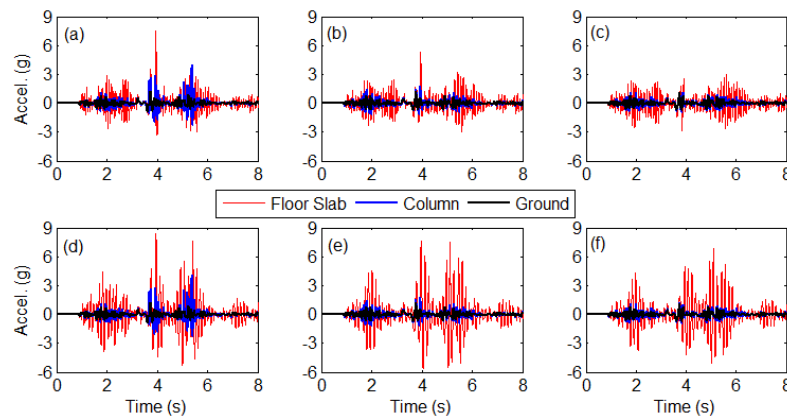

Figure 2.1. Vertical acceleration history at the middle of the floor slab, at the columns (average of several sensors), and at the shaking table (average of sensors) for 3D RRS for (a,d) TPB isolated configuration, (b,e) LRB/CLB isolated configuration, and (c,f) fixed-base configuration; (a-c) = 5th floor slab and (d-f) = roof slab.

3. AMPLIFICATION OF HORIZONTAL FLOOR ACCELERATIONS IN 3D MOTIONS

While the ceiling damage as described above has been attributed primarily to vertical slab vibration occurring in significant vertical ground excitation, horizontal floor accelerations were also amplified during 3D excitation compared to XY excitation. For direct comparison of the influence of strong vertical excitation, the RRS excitation was repeated in each building configuration with 3D and XY excitation. Figure 3.1 compares the y-direction horizontal accelerations at the building center (averaged from the SE and NW column sensors) from the XY and 3D RRS excitations at 5th and roof slabs for each system configuration over the most intense part of the record. For both the TPB and LRB/CLB isolated buildings, the horizontal accelerations increase from values less than 0.5g in XY excitation to around 1g in 3D excitation [Fig. 3.1(a,b,d,e)]. The amplification appears to be caused by high frequency vibration (around 7-10 Hz) that is not present during XY excitation, and suggests a lateral-vertical coupling effect that reduces the benefit of seismic isolation for this particular excitation. A similar high frequency component is also present in the accelerations of the fixed-base building [Fig. 3.1(c,f)], but its amplitude is smaller and its influence is diminished by the fact that the horizontal accelerations are already large (around 1g) under XY excitation.

The characteristic high frequency vibration and subsequent amplification of horizontal acceleration was replicated in accelerometers throughout the building in each of the system configurations. To convey the big picture, the profile of peak horizontal acceleration observed during the RRS excitation
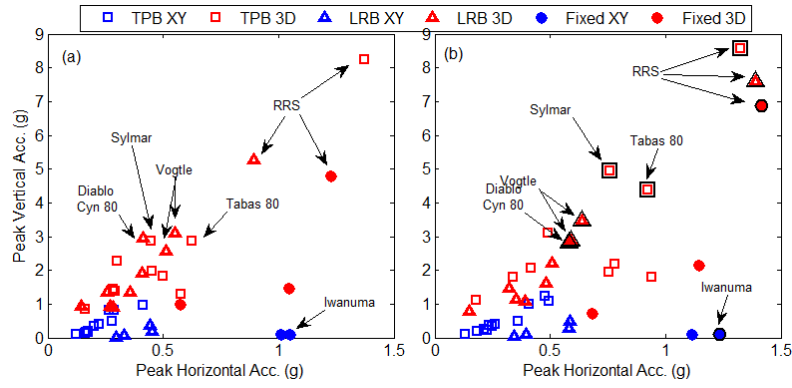
Figure 2.2. Peak vector horizontal acceleration vs. peak vertical acceleration at (a) 4th ceiling level and (b) 5th ceiling level for each test run; blue = XY excitations and red = 3D excitations; motions causing moderate or worse ceiling damage outlined in black.

is compared for each system configuration for XY excitation [Fig. 3.2(a)] and for 3D excitation [Fig. 3.2(b)]. The figures include absolute acceleration and acceleration normalized by horizontal peak ground acceleration (H-PGA) so that the level of attenuation may be better observed. During XY excitation [Fig. 3.2(a)], the isolation systems performed as expected, keeping accelerations below about 0.5g and distributed essentially uniformly over height. Peak accelerations are observed to be slightly lower in the TPB isolated building than in the LRB/CLB isolated building, which is a reflection of the relative design parameters of the isolation systems. Accelerations in the fixed-base building are somewhat larger than both isolated building configurations, even though the horizontal input acceleration was scaled to 40% of that applied to the isolated buildings. The normalized plot shows that accelerations are attenuated by more than a factor of 2 in the isolated buildings and amplified by a factor of 2.5 in the fixed-base building.
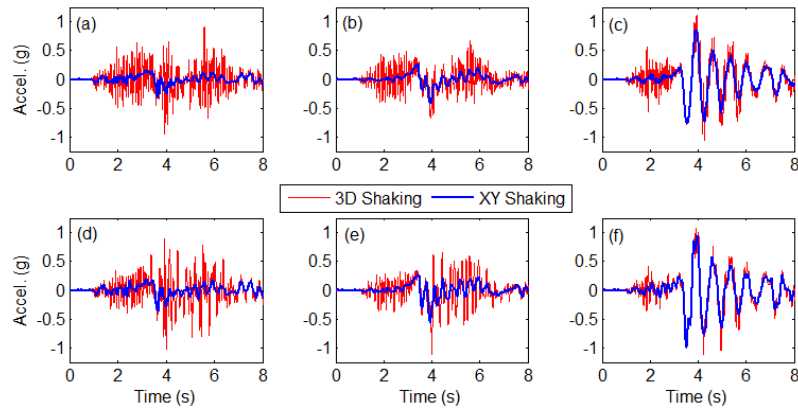

Figure 3.1. Y-direction horizontal floor acceleration history (average of instrumented columns) compared for 3D and XY RRS test motion for (a,d) TPB isolated configuration, (b,e) LRB/CLB isolated configuration, and (c,f) fixed-base configuration; (a-c) = 5th floor slab and (d-f) = roof slab.

The peak acceleration in all building configurations is amplified in 3D excitation [Fig. 3.2(b)] compared to XY excitation. This amplification is relatively small in the fixed-base building, but more significant in the isolated building configurations. The amplification is somewhat larger in the TPB configuration compared to the LRB/CLB configuration. Average acceleration amplification factors for each configuration are: 3.37 for TPB isolated building, 2.1 for LRB/CLB isolated building, and 1.15 for fixed-base building. Despite the observed amplification, the normalized plot emphasizes that attenuation of the ground acceleration is still present in the isolated buildings; that is, the peak floor accelerations are generally less than PGA. In the fixed-base building, on the other hand, H-PGA is amplified by nearly a factor of 3 at the roof level.
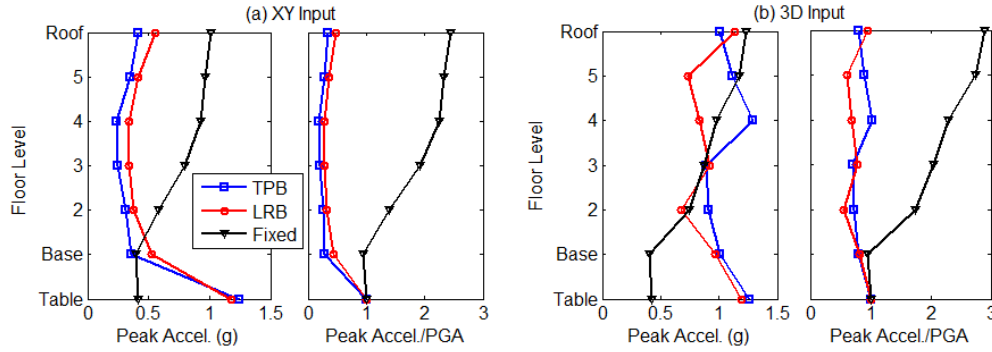
Figure 3.2. Peak floor acceleration (vector sum of x and y-components, average of instrumented columns) vs. floor level for RRS test motion: (a) XY excitation and (b) 3D excitation. Accelerations are absolute on the left graph and normalized by PGA on the right graph.

The RRS 3D excitation replicated by the table represents an example of extreme vertical ground acceleration. Although no other direct comparisons between XY and 3D excitation were generated, the data from all test runs suggests that horizontal floor accelerations were amplified whenever vertical ground shaking was present, and the intensity of the amplification was closely related to the intensity of the vertical component. The influence of the vertical component of shaking on horizontal ground acceleration attenuation is complicated by the fact that isolation systems are more effective in stronger horizontal ground motions. This point is illustrated in Figure 3.3, which shows a spatial plot of the attenuation ratio (peak floor acceleration/H-PGA) against H-PGA and V-PGA for all the trials in the isolated building configuration. The attenuation ratio is projected vertically from the base plane of the graph. Figure 3.3(a) illustrates that the attenuation ratio tends to increase as V-PGA increases; in other words, the reduction in floor acceleration relative to H-PGA is somewhat diminished as V-PGA increases. On the other hand, Fig. 3.3(b) illustrates that the attenuation ratio tends to decrease as H-PGA increases; that is, floor accelerations are further reduced relative to H-PGA as H-PGA increases in intensity. From this, one can surmise that for most levels of vertical input, the isolation system still achieves its intended effect.
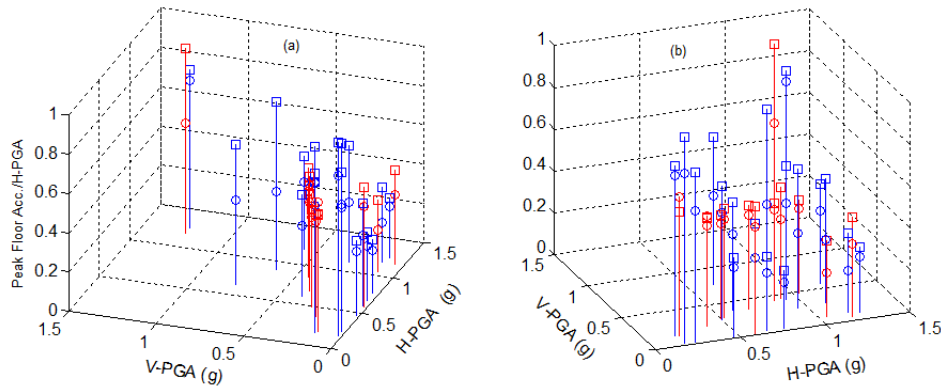

Figure 3.3. Acceleration attenuation ratio (peak floor acceleration/H-PGA) versus H-PGA and V-PGA. Blue = TPB system, red = LRB/CLB system; ○ = 5th floor slab, □ = roof slab. (a) and (b) show the same data from different perspectives.

4. EXPLANATION OF HORIZONAL-VERTICAL COUPLING

The trends observed in the test data suggest that some form of horizontal-vertical coupling was present in the building specimen, and was stronger in the isolated building configurations. These trends have been confirmed by numerical modeling and analysis of the test building to the input table motions.

The analytical model of the building uses displacement-based nonlinear frame elements to model the beams and columns, discretized into 3 elements for each column and several elements for each beam or girder. The influence of floor slabs is accounted for through composite sections for the beams and girders, and mass is distributed to individual nodes across the floor spans. Bidirectionally coupled plasticity models are used to describe both TPB and LRB response, and the interaction between shear resistance and axial force of the TPBs is included. The analytical models for each building configuration replicate the essential features of the response characteristics with a high degree of fidelity. These analytical models have also been used to explore additional scenarios not represented in the test data. Through this investigation, two major sources of horizontal-vertical coupling have been identified, which are described in the following sub-sections. The coupling theory is justified primarily by supporting test data at this time, while details of the analytical modeling and numerical studies will be presented in future publications.

4.1. Horizontal-Vertical Coupling of Mode Shapes in the Building Specimen

The first source of horizontal acceleration amplification is a horizontal-vertical coupling of the modes in the building specimen, or horizontal movement in the vertical modes of the structure. Figure 4.1 illustrates the primary vertical mode of the LRB/CLB isolated building (TPB building is similar) and the fixed-base building, as determined by modal analysis of the analytical models. The described modal coupling shows up primarily in the y-direction. In the isolated building [Fig. 4.1(a)], horizontal motion is strongest at the base, 3rd and 4th floors, while the horizontal motion is close to zero in the 2nd and 5th floors. Thus, the 2nd and 5th floors can be considered to be nodes in the primary vertical mode. According to the model, this first vertical mode at 7 Hz comprises about 40% of the mass participation in the vertical direction. The mode shape of the fixed-base building [Fig. 4.1(b)] is shifted since horizontal motion is constrained at the base; a node appears at about the 4th floor.

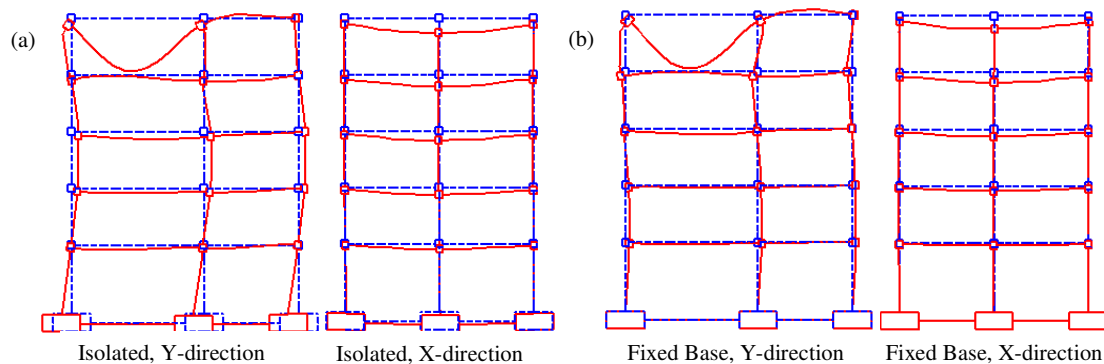| Isolated, Y-direction | Isolated, X-direction | Fixed Base, Y-direction | Fixed Base, X-direction |

Figure 4.1. Primary vertical mode shape in (a) LRB/CLB isolated building (7.0 Hz) and (b) fixed-base building (7.06 Hz). Horizontal degrees of freedom are activated in these mode shapes.

The test data strongly supports the occurrence of modal coupling in the TPB isolated building. While the RRS ground motion was an extreme example, Fig. 4.2 shows select acceleration data for a representative XY excitation – 80% of ChiChi-TCU065 – and a representative 3D excitation -100% of Kobe-Takatori. Note that the realized peak table accelerations were similar in the horizontal direction for each of these motions (H-PGA = 0.77g for Chi-Chi and 0.95 for Takatori), while the vertical input for Takatori was moderate (V-PGA = 0.27g). Shown in Figure 4.2 are floor acceleration histories and floor spectra at the roof level, as well as peak acceleration profiles over the height of the building, both absolute and normalized by H-PGA. The amplitude of the roof accelerations is quite a bit higher for Takatori, and higher frequency content appears in the acceleration history. Local peaks appear in the roof spectra for each motion at the following frequencies: 1) range of 1.5-3.0 sec, which indicates the variable isolation period, 2) 0.3-0.4 sec, which is the first horizontal structural mode, and 3) 0.17 sec, which is the vertical mode shown in Fig. 4.1. While the contribution to the floor spectra at 0.17 sec is minimal for the ChiChi (XY) excitation, it represents the most dominant peak for Takatori (3D) input

in the x-direction, which has peak roof acceleration > 0.5g. Clearly, the contribution of the fundamental vertical mode in the horizontal acceleration is significant.

As further evidence, the peak acceleration profiles show that for ChiChi (XY) excitation, the distribution of peak floor acceleration is nearly uniform with height, as expected, and the floor accelerations are attenuated to about 25% of H-PGA, showing the great effectiveness of the isolation system. For the Takatori (3D) input, on the other hand, the peak acceleration profile is not uniform with height, but instead has local minima at the 2nd and 5th floors, which are the *same floors* that corresponded to nodes in the primary vertical mode (Fig. 4.1). Interestingly, the vertical mode shape in Takatori is strong in the x-direction while modal coupling is expected primarily in the y-direction; however, several of the tests showed this type of acceleration profile trend in both x and y-direction. Although the vertical mode contributes to the horizontal response, it does not override the effect of isolation for this vertical input, as the input acceleration still attenuated to 35-60% of H-PGA. Furthermore, Takatori is a very difficult motion to isolate against because of the large pulse in the range of 2-3 seconds, and the TPB system as designed accommodated this motion easily.
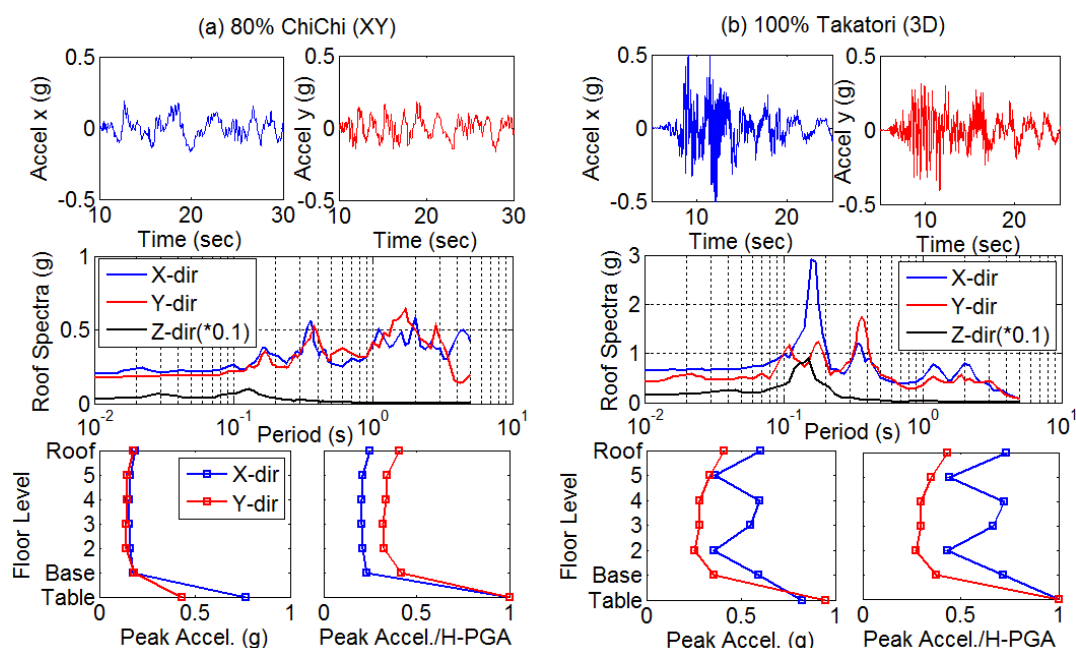

Figure 4.2. Floor accelerations at roof level, floor spectral accelerations at roof level, and peak acceleration profiles in TPB isolated building for (a) 80% ChiChi (XY) and (b) 100% Takatori (3D)

Figures 3.1 and 3.2 show evidence of strong modal coupling in the LRB/CLB system under the extreme RRS input. A more representative example for this system (Fig. 4.3) suggests that in general, the coupling is not as strong as in the TPB system. In Fig. 4.3, acceleration data are compared for the Diablo Canyon motion, which was run at 95% scale factor for XY excitation, and 80% scale factor for 3D excitation. The realized table accelerations for these motions were H-PGA = 1.12g for 95% XY excitation and 0.91g for 80% 3D excitation (x-direction), while the vertical component for 3D excitation was V-PGA = 0.45g. From Fig. 4.3, coupling in the x-direction appears to be absent, as the frequency content in the roof acceleration histories are visually identical for 95% XY and 80% 3D excitation, and the vertical mode does not show up in the x-direction roof spectra or acceleration profiles. The vertical mode is moderately apparent in the y-direction roof acceleration history [Fig. 4.3(b)], but some discrepancies are observed that are difficult to interpret. First, the amplified frequency content for the horizontal direction does not exactly align with the fundamental vertical mode frequency. Second, the acceleration profile shows reduction only at the 2nd floor and is further amplified at the roof. Both of these trends were observed throughout the test series, and further investigation of the coupling phenomena in the LRB/CLB system is needed to understand them. The

effect of the y-direction modal coupling is to increase the attenuation ratios from an average of 30% of H-PGA to 50% of H-PGA, again preserving the overall effectiveness of the isolation system.
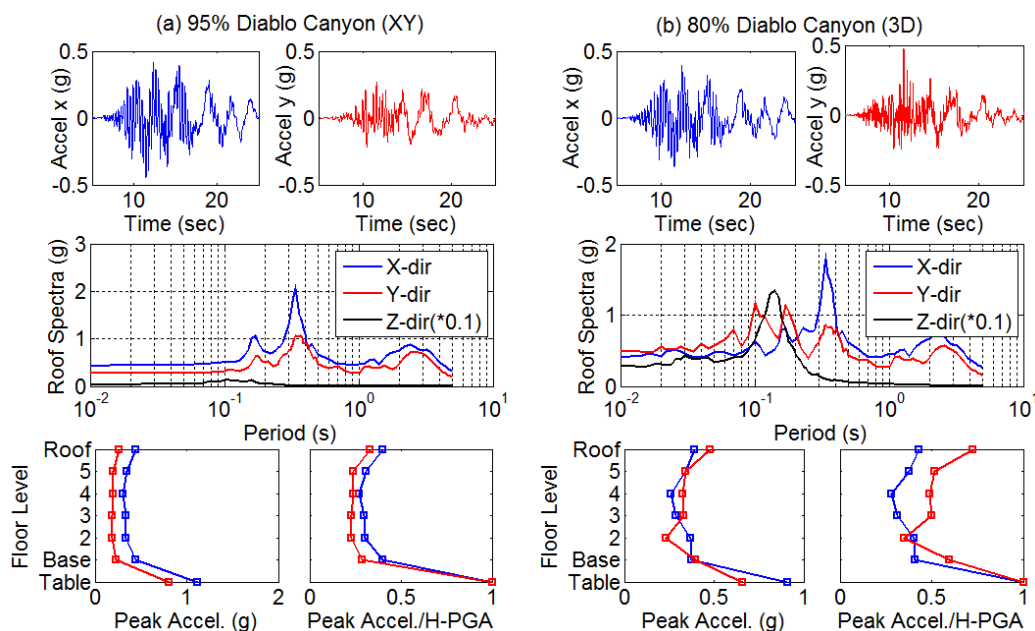

Figure 4.3. Floor accelerations at roof level, floor spectral accelerations at roof level, and peak acceleration profiles (y-direction only) in LRB/CLB isolated building for (a) 95% Diablo Canyon (XY) and (b) 80% Diablo Canyon (3D)

The only test data available to assess modal coupling in the fixed-base building is the extreme RRS example. Floor acceleration histories and peak acceleration profiles for this case were already shown (Figs 3.1 and 3.2) and the roof spectra are shown in Fig. 4.4. As described previously, the high frequency amplification of the horizontal acceleration (contribution of the fundamental vertical mode) appears to be present though obscured by the more dominant fundamental horizontal mode. In the peak acceleration profile for 3D excitation [Fig. 3.2(b)], this shows up as a reduction in the 4th floor peak – a node in the fundamental vertical mode – relative to the acceleration profile for XY excitation. The vertical mode is mildly present in the y-direction roof spectra for 3D excitation [Fig. 4.4(b)].
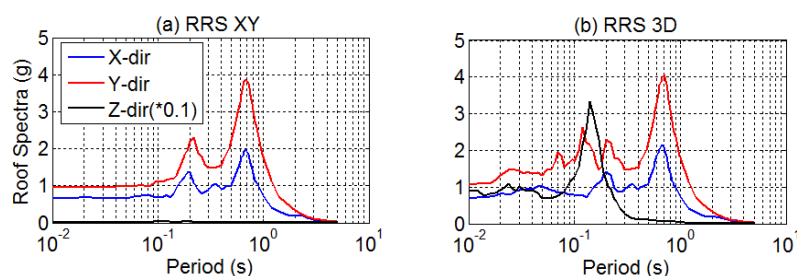

Figure 4.4. Roof spectral accelerations in fixed-base building for (a) 35% RRS (XY) and (b) 35% RRS (3D)

4.2. Axial-Shear Force Interaction in Friction Isolators

Another significant source of horizontal-vertical coupling in the TPB isolation system is the direct relation between the axial load and horizontal shear force of friction devices. In any friction bearing, the horizontal force generated in the bearing is proportional to the axial load carried on the bearing. The influence of axial load on the total base shear of the system in the RRS motion is presented in Fig. 4.5, which compares base shear and total axial force for XY and 3D excitation. Observe that for XY

excitation, the total axial force on the TPB system was essentially constant, and thus the total base shear was unaffected by localized axial force variation and contains only low frequency oscillations [Fig. 4.5(a)]. However, under the extreme vertical acceleration (>1g) that occurred during 3D excitation, the total axial force on the TPB system varied from 0 to more than 3 times the weight of the building. Thus, the shear force generated in the isolation system more than doubled when instances of large shear force coincided with instances of peak axial force. Furthermore, the high frequency axial force variation (coincident with the dominant vertical frequency of the structure) introduced a high frequency component into the shear force that naturally propagated through the structure. In addition to the structural modal coupling described earlier, this base input likely amplified the response in other horizontal structural modes with frequencies close to the vertical mode frequency.
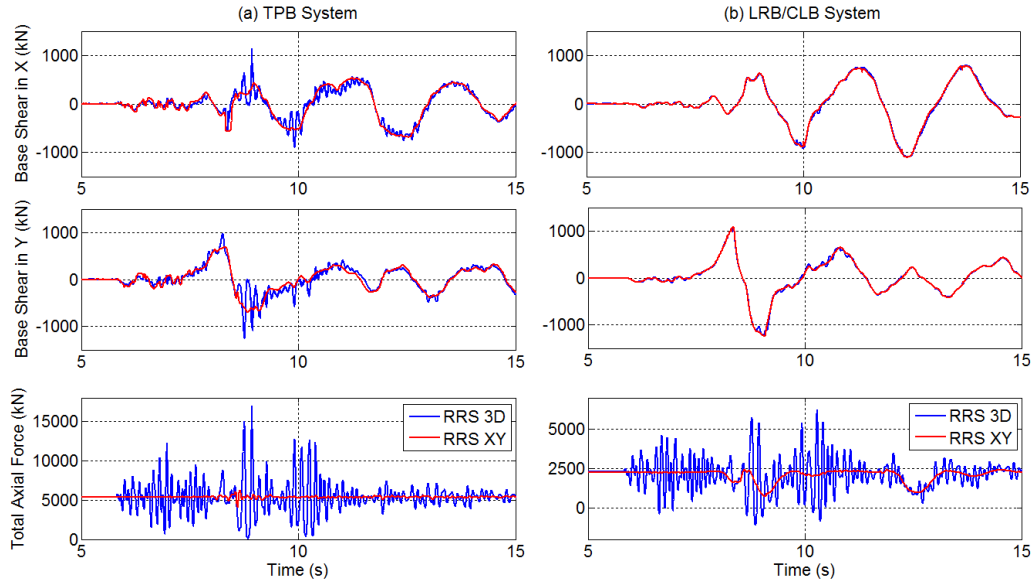

Figure 4.5. Total x and y-direction shear force and total axial force for (a) all 9 isolators of TPB system and (b) 4 LRBs for LRB/CLB system, compared for RRS XY and RRS 3D excitation.

Axial force-shear force interaction can also occur in elastomeric bearings. For instance, previous sources (e.g. Kelly 1997) have noted that at large displacements, elastomeric bearings suffer a loss of axial load carrying capacity, and the horizontal stiffness decreases as the axial load on the bearing approaches the critical load. This axial-shear interaction is not likely to be significant unless the bearings approach their stability limits. For comparison, the total base shear in the LRBs for the LRB/CLB system is plotted for XY and 3D excitation in Fig. 4.5(b). This figure indicates only a slight difference in the base shear for 3D excitation compared to XY excitation, despite a similar variation in bearing axial force. This suggests that horizontal-vertical coupling introduced to the system through the LRB devices was minor, and explains why the LRB/CLB system experienced reduced amplification of horizontal floor accelerations relative to the TPB system. Incidentally, Fig. 4.5(b) includes axial forces on the 4 LRBs only, showing that a net transfer of axial force between LRBs and CLBS occurred several times during the excitation.

5. DISCUSSION AND CONCLUDING REMARKS

The influence of both moderate and extreme vertical excitation on the response of a full-scale base building with two different base-isolation systems and in the fixed-base configuration has been presented. Damage to suspended ceilings occurred under the combination of horizontal floor accelerations > 0.5g and vertical slab acceleration > 3g. The horizontal floor accelerations were amplified in 3D excitation compared to XY (horizontal only) input due to a horizontal-vertical modal

coupling of the asymmetric structure and axial-shear force interaction in friction isolation devices.

Peculiarities of the experiment likely exaggerated the vertical slab vibration and horizontal-vertical coupling compared to a typical structure. For instance, the supplementary mass at the roof level (Sasaki et al. 2012) amplified the intensity of vertical vibration at the roof level and may have amplified the horizontal coupling in the fundamental vertical mode. (The roof slab was designed for supplementary mass representative of roof mounted equipment and/or a penthouse.) Furthermore, the modal coupling in the structure should disappear in buildings that are symmetric. However, many structures have irregularities, such that modal coupling should be considered on a case-by-case basis.

In conclusion, we emphasize that horizontal-vertical coupling did not compromise the ability of the isolation systems to significantly attenuate the horizontal floor accelerations relative to the ground accelerations, and protect the structural system entirely from damage. Vertical slab acceleration appeared to be a more dominant factor than horizontal floor acceleration in the non-structural damage that was observed. This evidence suggests that the influence and mitigation of vertical ground acceleration should be realistically considered in the design and analysis of structures with continued functionality performance objectives.

REFERENCES

Clark, P.W., Kelly, J.M. (1990). Experimental testing of the resilient-friction base isolation system, *Report No. UCB/EERC-90/10*, Earthquake Engineering Research Center, University of California, Berkeley, CA.

Fenz, D.M. and Constantinou, M.C. (2008). Development, implementation, and verification of dynamic analysis models for multi-spherical sliding bearings", *Technical Report MCEER-08-0018*, MCEER, State University of New York at Buffalo, Buffalo, NY, USA.

Hwang, J.-S., Hsu, T.-Y. (2000). Experimental study of isolated building under triaxial ground excitations, *ASCE J. Struct. Eng.* **126:8**, 879-886.

Juhn, G., Manolis, G., Constantinou, M.C., Reinhorn, A.M. (1992). Experimental investigation of secondary systems in a base-isolated structure, *J. Struct. Eng.* **118:8**, 2204-2221.

Kelly, J.M. (1997). *Earthquake resistant design with rubber.* Springer.

Kelly, J.M., Tsai, H.C. (1985). Seismic response of light internal equipment in base-isolated structures, *Earthquake Engng Struct. Dyn.* **13:6**, 711-732.

Okazaki, T., Sato, K., Sato, E., Sasaki, T., Kajiwara, K., Ryan, K. and, Mahin, S. (2012). NEES/E-Defense base isolation tests: perfomance of triple-pendulum bearings, *Proc. 15th World Conf. on Earthquake Engin.*

Ryan, K.L., Dao, N.D., Sato, E., Sasaki, T., Okazaki, T. (2012). Aspects of isolation device behavior observed from full-scale testing of an isolated building at E-Defense, *Proc. ASCE Structures Congress*, Chicago, IL.

Sasaki, T., Sato, E., Ryan, K. L., Okazaki, T., Mahin, S. and Kajiwara, K. (2012). NEES/E-Defense base isolation tests: effectiveness of friction pendulum and lead-rubber bearing systems, *Proc. 15th World Conf. on Earthquake Engng.*

Sato, E., Furukawa, S., Kakehi, A., Nakashima, M. (2011). Full-scale shaking table test for examination of safety and functionality of base-isolated medical facilities, *Earthquake Engng Struct. Dyn.* **40:13**, 1435-1453.

Soroushian et al. (2012). NEES/E-Defense tests: seismic performance of ceiling/partition/sprinkler piping nonstructural systems in base isolated and fixed base building, *Proc. 15th World Conf. on Earthquake Engng.*

Tagawa, Y. and Kajiwara, K. (2007). Controller development for the E-Defense shaking table, Proc. IMechE Vol. 221, Part I, *J. Systems and Control Engineering*.

Wolff, E.D., Constantinou, M.C. (2004). Experimental study of seismic isolation systems with emphasis on secondary system response and verification of accuracy of dynamic response history analysis methods, *Technical Report MCEER-04-0001*, MCEER, State University of New York at Buffalo, Buffalo, NY, USA.